

ARTICLE

Time-to-Event Modeling of Peripheral Neuropathy: Platform Analysis of Eight Valine-Citrulline-Monomethylauristatin E Antibody–Drug Conjugates

Matts Kågedal^{1,*†}, Divya Samineni^{1,†}, William R. Gillespie², Dan Lu¹, Bernard M. Fine¹, Sandhya Girish¹, Chunze Li¹ and Jin Y. Jin¹

Peripheral neuropathy (PN) is a common long-term debilitating toxicity of antimicrotubule agents. PN was the most frequent adverse event resulting in dose modifications and/or discontinuation of treatment for valine-citrulline-monomethylauristatin E antibody–drug conjugates (ADCs) developed at Genentech. A pooled time-to-event analysis across eight ADCs (~700 patients) was performed to evaluate the relationship between the ADC exposure and the risk for developing a clinically significant (grade ≥ 2) PN. In addition, the impact of demographic and pathophysiological risk factors on the risk for PN was explored. The time-to-event analysis suggested that the development of PN risk increased with ADC exposure, treatment duration, body weight, and previously reported PN. This model can be used to inform clinical strategies such as adaptations to dosing regimen and/or treatment duration as well as inform clinical eligibility to reduce the incidence of grade ≥ 2 PN.

Study Highlights

WHAT IS THE CURRENT KNOWLEDGE ON THE TOPIC?

✓ Peripheral neuropathy (PN) is a frequent adverse event resulting in dose modifications and/or treatment discontinuations for valine-citrulline-monomethylauristatin E antibody–drug conjugates (ADCs).

WHAT QUESTION DID THIS STUDY ADDRESS?

✓ What are the important patient risk factors for developing PN? Does the ADC target or cancer type influence the risk? What are the relevant treatment options considering the risk for PN?

WHAT DOES THIS STUDY ADD TO OUR KNOWLEDGE?

✓ Prior PN and body weight appear to be the most important risk factors in addition to dose and treatment duration. Drug target and cancer type do not seem to play an important role.

HOW MIGHT THIS CHANGE DRUG DISCOVERY, DEVELOPMENT, AND/OR THERAPEUTICS?

✓ The developed-to-event model can be used to inform clinical strategies such as adaptations to dosing regimen and/or treatment duration as well as inform clinical eligibility to reduce the incidence of grade ≥ 2 PN.

With recent advances in cancer diagnosis and treatment, the overall cancer death rate in the United States has declined by 1.5% annually during the past decade, resulting in an estimated 15.5 million cancer survivors in 2017.¹ Although an increasing number of cancer patients become long-term survivors, these survivors endure physiological sequelae and side effects from the disease and its treatments that can potentially interfere with the completion of treatment and negatively impact cancer survivors' quality of life. Therefore, oncology therapeutics need to be optimized to enhance the benefit–risk profile for patients through rational dose/dose regimen selection.

Amongst the most debilitating of these long-term toxicities is chemotherapy-induced peripheral neuropathy (PN) that can lead to permanent symptoms and disability in up to 38% of cancer survivors.^{2,3} PN is a common nonhematological

adverse event associated with a number of effective chemotherapeutic agents, including platinum compounds,^{4,5} taxanes,^{6,7} vinca alkaloids,^{8,9} thalidomide, and bortezomib. PN affects distinct components of the nervous system, from the sensory cell bodies in the dorsal root ganglion to the distal axons of the primary sensory neurons, leading to paresthesia, dysesthesia, and numbness in the hands and feet.¹⁰ The clinical presentation of PN is predominantly sensory, rather than motor, with symptoms predominantly occurring in a cumulative dose-dependent manner, with a symmetric, distal, length-dependent “stocking-glove” distribution.¹¹ The risk profiles vary depending on the mechanisms of neurotoxicity among the different offending agents, dose intensity, duration of exposure, and the site of action.^{12,13} PN has the potential to interfere with treatment by compromising treatment

[†]Contributed equally.

¹Genentech Inc., South San Francisco, California, USA; ²Metrum Research Group LLC, Tariffville, Connecticut, USA. *Correspondence: Matts Kågedal (kagedal.matts@gene.com)

Received: February 20, 2019; accepted: May 1, 2019. doi:10.1002/psp4.12442

adherence and by limiting the dosing intensity of long-term treatment, resulting in reduced efficacy.

Antibody–drug conjugates (ADCs) constitute a sophisticated class of therapeutic agents that allow delivery of highly potent antineoplastic agents to target cells via specific antibody–antigen binding while minimizing exposure to healthy cells.¹⁴ The valine-citrulline-monomethylauristatin E (vc-MMAE) class of ADCs constitute the largest group of ADCs in clinical development.¹⁵ MMAE is a synthetic auristatin derivative that inhibits cell division and promotes apoptosis by disrupting the microtubule network upon binding to tubulin.¹⁶ These ADCs use a protease-labile linker, maleimidocaproyl valine citrulline p-aminobenzyloxycarbonyl, conjugated to a potent antimetabolic agent, monomethyl auristatin E (MMAE) via solvent accessible thiols present in monoclonal antibody (mAb) cysteines (vc-MMAE ADC). Although the Genentech (South San Francisco, CA) vc-MMAE ADCs target different tumor-specific antigens against a wide variety of cancer types, i.e., solid tumors and/or hematological malignancies, they use the same linker-drug combination (i.e., vc-MMAE).

In clinical studies (phases I and II) conducted with eight vc-MMAE ADCs developed at Genentech, PN was the most frequent adverse event resulting in dose modification and treatment discontinuation. This is consistent with the clinically observed adverse event profile following the administration of brentuximab vedotin, a vc-MMAE-containing ADC targeting the cancer antigen CD30, in lymphoma patients.^{17–19} The pharmacokinetics (PK) of the antibody-conjugated monomethyl auristatin E (ac-MMAE, measured as MMAE conjugated to the mAb) analyte have previously been shown to be largely comparable across the eight vc-MMAE ADCs in a pooled analysis.²⁰ The intercompound variabilities were estimated to be 15% and 5% for clearance and central volume of distribution, respectively, which are small compared with the corresponding interpatient variabilities of 39% and 15%. Clinical results from all eight ADCs included here have previously been published individually.^{21–28}

Exploratory exposure–safety evaluations for the individual vc-MMAE ADCs suggested that a higher exposure for the conjugate analyte was associated with a higher incidence of clinically significant (grade ≥ 2) PN. On the other hand, consistent with previous reports,²⁹ no correlation between unconjugated MMAE exposure and grade ≥ 2 PN was seen. A time-to-event (TTE) model was previously developed for polatuzumab vedotin, a vc-MMAE-containing ADC, to quantify the relationship between ADC exposure (MMAE conjugated to the mAb) and treatment duration on the incidence of PN, considering the cumulative onset of grade ≥ 2 PN events.³⁰ Given that the eight in-house vc-MMAE ADCs contain the same antimicrotubule agent (i.e., MMAE), display comparable PK properties, and have consistent exposure–response trends for grade ≥ 2 PN for the individual ADCs, we have performed a pooled TTE analysis to describe the exposure–safety relationships of grade ≥ 2 PN. This enabled an informative analysis despite limited data on each separate ADC (except polatuzumab) and also allowed a comparison among ADCs after accounting for other covariate effects. In fact, the developed TTE analysis leveraged a rich data set consisting of ~ 700 patients across the eight individual ADCs in phases I and II of clinical development.

Our objectives were as follows: (i) to evaluate the relationship between the ADC exposure and treatment duration on the clinically significant (grade ≥ 2) PN risk, (ii) to evaluate the impact of baseline demographic and pathophysiological risk factors on the PN risk, and (iii) to explore management/risk mitigation strategies (i.e., dose adaptations, capping of treatment duration, inform clinical eligibility) to reduce the incidence of grade ≥ 2 PN for in-house vc-MMAE ADCs in development.

METHODS

Study designs and data

The TTE analysis was based on the clinical data obtained following the administration of the eight in-house vc-MMAE ADCs evaluated in nine phase I and II studies of 694 cancer patients. The drug antigen targets, indications, number of patients, doses, and schedules for each ADC are summarized in **Table S2**. All studies were approved by the medical ethics committee and were carried out according to the International Conference on Harmonization guidelines for good clinical practice.³¹ The eight phase I monotherapy studies included both dose escalation and at least one expansion cohort at a dose identified for further clinical development. The doses tested in phase I were in the range 0.1–3.2 mg/kg administered every 3 weeks (q3w) and in the range of 0.8–1.6 mg/kg administered in a weekly regimen. All studies included an expansion cohort at 2.4 mg/kg, q3w. In addition, pinatuzumab vedotin (1.8 mg/kg q3w and 2.4 mg/kg q3w) and polatuzumab vedotin (2.4 mg/kg q3w) were also evaluated in combination with rituximab during the phase Ib portion of clinical development. In the phase II study, relapsed/refractory non-Hodgkin lymphoma patients were randomized to receive either 2.4 mg/kg q3w of pinatuzumab vedotin or 2.4 mg/kg q3w of polatuzumab vedotin in combination with rituximab, which has established clinical activity in B-cell malignancies. In addition, a cohort of follicular lymphoma patients received 1.8 mg/kg q3w of polatuzumab vedotin in combination with rituximab.

The PK collection was extensive, with multiple samples ($\sim n = 10$) collected during cycle 1 (up to 21 days post first dose) and 4–5 samples/cycle up to cycle 4. In addition, PK samples preinfusion and postinfusion were collected until cycle 8. No PK data were available for study DNB4987G at the time of the present analysis. For the remaining studies, 91% of the patients had PK observations and were also included in the previously reported population PK analysis.²⁰

Bioanalytical methods for PK concentrations of the ac-MMAE analyte

The concentration of the conjugate represented the total concentration of ac-MMAE conjugated to the antibody via the maleimidocaproyl-valine-citrulline-p-aminobenzyloxycarbonyl (MC-VC_PAB) linker. The conjugate concentrations for each ADC were measured in the plasma samples using a validated electrospray liquid chromatography-tandem mass spectrometry assay. Initially, affinity capture using protein A was used to capture the ADC followed by the enzyme-mediated release of MMAE and subsequent detection using liquid chromatography-tandem mass spectrometry.³² The lower limit of quantitation for validated

conjugate assays in human Li-heparin plasma across the eight programs was 0.179 ng/mL (0.25 nM) or 0.359 ng/mL (0.5 nM) with a linear range up to 35.9 ng/mL (50 nM) using a sample volume of 50 μ L.

Base model development

The individually predicted ac-MMAE concentration time course in plasma was used as an input function in the model. The individual PK profiles were derived based on a previously published pooled population PK analysis of the same studies.²⁰ The individual predictions for one of the patients was unrealistic with a clearance estimate at only ~3% of the expected value and a poor individual fit, most likely the result of inaccurate dosing history. This patient was excluded from the analysis. For patients not included in the PK analysis, the population PK parameter estimates were used to predict individual exposures accounting for covariate effects.

The TTE model for grade ≥ 2 PN published previously for polatuzumab vedotin³⁰ was used as a starting point. The addition of a transit compartment between plasma and the effect compartment provided a slightly better fit to the data with the same number of parameters. Hence, in the final base model, the delay between start of treatment and the increased incidence of grade ≥ 2 PN was described by a transit compartment ($C_{transit}$) followed by an effect compartment where the first order transit rate constant (Ktr) determines the extent of the delay (**Figure 1**). A linear relationship between drug concentration in the effect compartment (C_e) and the drug effect (E_{drug}) was assumed where α was the estimate slope. An EMAX model was also tried but did not improve the fit. A Weibull function was also included in the final base hazard model, including the parameter β to further allow a time-varying baseline hazard (h_{base}). The model appropriately accounted for right censoring for patients who discontinued the study or died prior to experiencing grade ≥ 2 PN. The structure of the final base model is illustrated in **Figure 1** and specified in Eqs. 1–4, where t is time.

$$\frac{dC_{transit}}{dt} = Ktr \cdot C_p(t) - Ktr \cdot C_{transit}(t) \quad (1)$$

$$\frac{dC_e}{dt} = Ktr \cdot C_{transit}(t) - Ktr \cdot C_e(t) \quad (2)$$

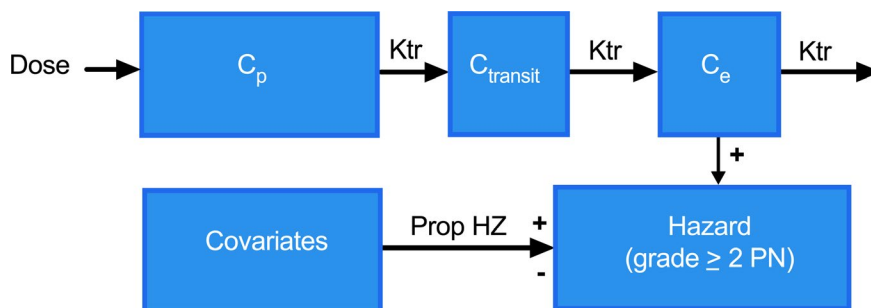


Figure 1. Model structure. The hazard in the time-to-event model is driven by individually predicted antibody–drug conjugate plasma concentrations (C_p). Transit and effect compartments were included to account for the slow initial event rate. The hazard was linearly related to the concentration in the effect compartment (C_e). In addition, a Weibull function on top of the drug effect on hazard is added for slight improvement over time. Covariates in the full and final models were included assuming proportional hazards (Prop HZ). Ktr, first order transit rate; $C_{transit}$, concentration in the transit compartment; PN, peripheral neuropathy.

$$E_{drug}(t) = \alpha \cdot C_e(t) \quad (3)$$

$$h_{base}(t) = \beta \cdot E_{drug}(t)^\beta \cdot t^{(\beta-1)} \text{ (Weibull function)} \quad (4)$$

The analysis was conducted using the NONMEM software version 7.3.0 (Icon Development Solutions, Ellicott City, MD).³³ Goodness of fit was evaluated based on evaluation of Kaplan–Meier visual predictive checks (VPCs). The VPCs were created by Monte Carlo simulations using Perl-speaks-NONMEM (PsN) 3.7.6 (number of simulated studies ≥ 300) and the Kaplan.plot function of Expose 4 for plotting.³⁴

Covariate analysis

The association between covariates of interest and the risk for development of PN were explored. Covariates were selected based on previously reported analyses²⁰ as well as scientific and clinical interests. Evaluated covariates included body weight (BWT), prior PN, albumin (ALBU), diabetes, performance status based on the response criteria of the Eastern Cooperative Oncology Group (ECOG), age, gender, prior chemotherapy treatment, concomitant rituximab treatment, ADC target, and cancer type. Four patients had missing BWT. The BWT for these patients were imputed as the median BWT of the corresponding sex.

Covariates were initially explored in a univariate fashion both by inspection of the VPCs from the base model and by introducing covariates one by one to the base model assuming proportional hazards. A full covariate model, including all covariates of interest except ADC target and cancer type, was also fit to the data to account for any correlations between covariates and to obtain accurate estimates of the imprecision.³⁵ In addition, backward elimination of insignificant covariates ($P = 0.05$) was performed to derive a final model. The different ADCs were studied in different cancer types, including prostate cancer and ovarian cancer, which are gender specific. The ADC target and cancer type were hence confounded with each other and also with gender to some extent. The inclusion of these covariates simultaneously in the full model was hence not possible. The potential influence of the ADC target and cancer type was therefore assessed after

developing a final covariate model based on the other covariates. BWT was selected as the metric for body size for the initial full model and covariate screening. Body mass index (BMI) is correlated with BWT and was therefore explored after development of the final model. Case deletion diagnostics³⁴ by trial was performed based on the final model to investigate if any study was particularly influential and to understand if any of the derived relationships could result from differences between trials. The effects of baseline covariates were introduced as proportional hazards as shown in Eq. 5.

$$h(t) = h_{\text{base}}(t) \cdot \exp(\theta_{\text{age}}(\text{age} - 65) + \theta_{\text{bwt}}(\text{BWT} - 75) + \theta_{\text{ALBU}}(\text{ALBU} - 4) + \theta_{\text{ECOG}}(\text{ECOG}) + \theta_{\text{female}}(\text{female}) + \theta_{\text{PPN}}(\text{PPN}) + \theta_{\text{Diabetes}}(\text{Diabetes}) + \theta_{\text{PriorChemo}}(\text{PriorChemo}) + \theta_{\text{ritux}}(\text{ritux})) \quad (5)$$

where $h_{\text{base}}(t)$ is the time varying hazard function described in Eq. 1. θ_{age} is the effect of age. θ_{bwt} is the effect of BWT.

θ_{ALBU} is the effect of ALBU (g/L). θ_{ECOG} is the effect of ECOG status (>0 vs. 0). θ_{female} is the effect of gender (female vs. male). θ_{PPN} is the effect of prior PN (yes/no); θ_{Diabetes} is the effect of diabetes (yes/no). $\theta_{\text{PriorChemo}}$ is the effect of prior chemotherapy treatment (yes/no), and θ_{ritux} is the effect of combining with rituximab (yes/no).

RESULTS

A base model was developed (Figure 1) that accounted for dosing history and individually predicted drug concentrations in plasma. It could describe the risk for developing PN over time as well as the exposure–response relationship (Figure 2). A univariate screen of baseline covariates of interest suggested that prior PN, high BWT, and male gender were associated with an increased risk for PN ($P < 0.05$). These trends could also be seen by inspection of the VPCs when simulating from the base model (not shown). Results

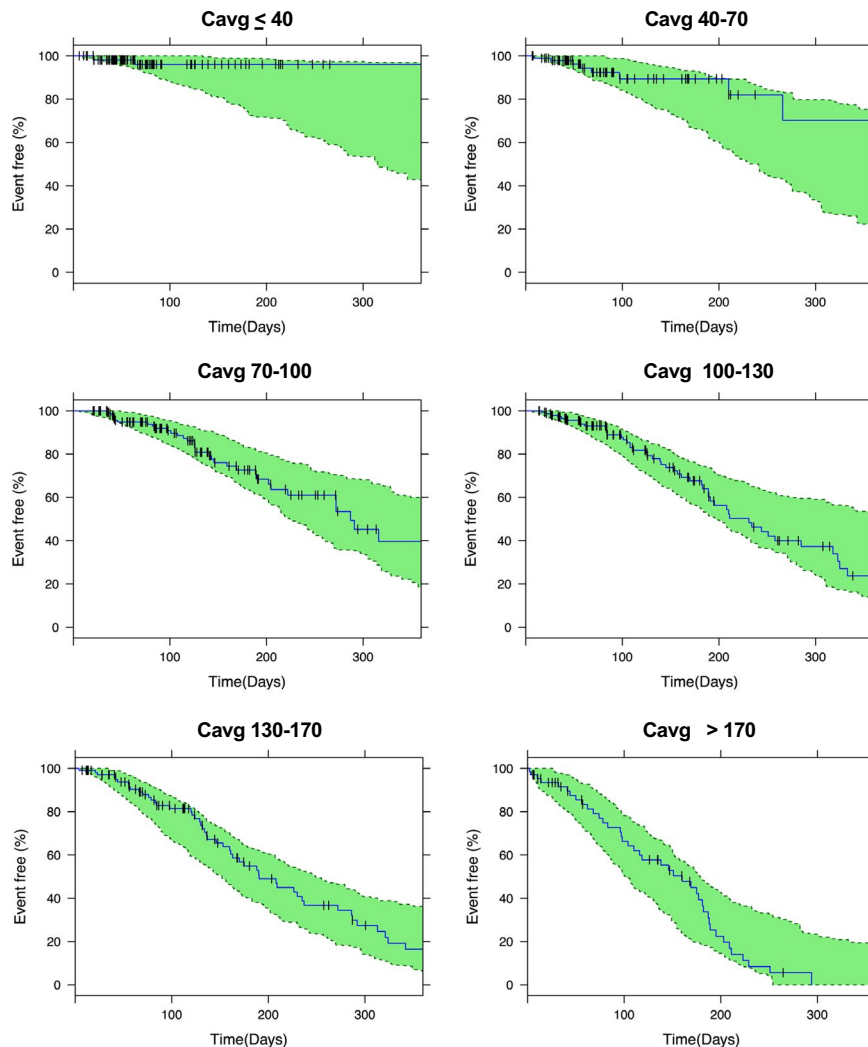


Figure 2. Base model Kaplan–Meier visual predictive check for time to grade ≥ 2 peripheral neuropathy at different levels of average plasma concentrations (C_{avg} ; ng/mL). C_{avg} was computed as the area under the curve up to the observed or simulated event divided by the time to the event.

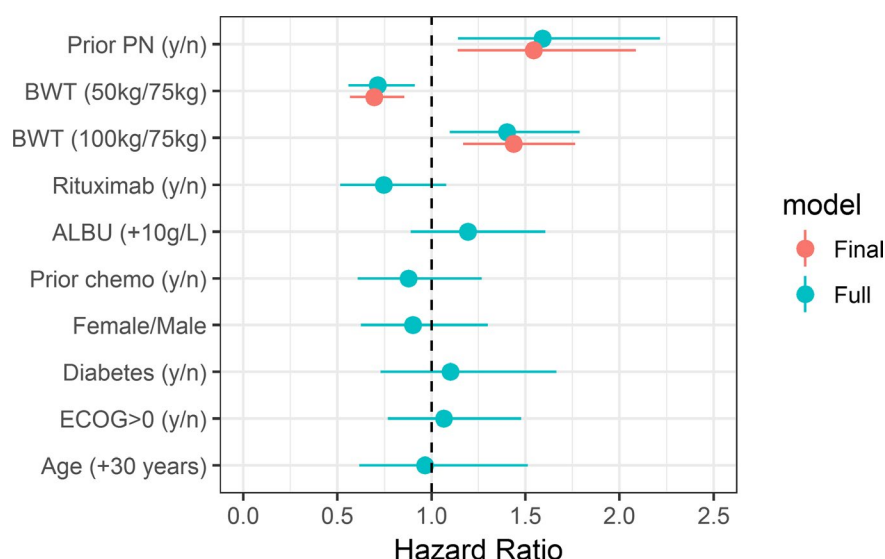


Figure 3. Estimated hazard ratios (95% CI) for covariate effects based on full and final model. ALBU, albumin; CI, confidence interval; BWT, body weight; ECOG, Eastern Cooperative Oncology Group; PN, peripheral neuropathy.

based on the full model, including all covariates except target and cancer type, suggested that BWT and prior PN were the most important covariates. However, there was no effect of gender (**Figure 3**). The gender difference seen in the univariate screen was hence explained by the differences in BWT between the male and female patients. Consistent with this finding, the final model, after backward elimination, only included prior PN and BWT. Obesity is a known risk factor for diabetic patients to develop PN.³⁶ It was therefore of interest to explore if BMI rather than BWT was responsible for the increased risk. Replacing BWT with BMI in the final model, however, resulted in a poorer fit (objective function value (OFV) increased by 5.6) and could not explain the gender effect. A hazard ratio of around 1.5 was seen for prior PN (yes/no) as well as for an increase in BWT of 30 kg. This finding was consistent for both the full and final models (**Figure 3**). The difference in the NONMEM OFV of 3.7 between the full and the final models was small considering that the full model contained five additional parameters. The parameter estimates of the full and final models were generally determined with an acceptable precision (**Table 1, Table S1**).

The VPCs based on the final model (**Figure S1**) illustrate that the initial delay in the onset of PN seen in the observed

data is captured well by the model. The model performed well for weekly as well as for q3w dosing, although the number of patients on weekly dosing was limited. Model predictions for patients with BWT greater or less than 75 kg with and without prior PN was also adequate (**Figure S2**).

The VPCs by tumor type/target based on the final model suggested that it could describe the individual tumor types well (**Figure 4**). Although the observed TTE was in the lower range predicted by the model for melanoma patients and in the upper range for ovarian patients, they are generally within the interval predicted by the model. Furthermore, the addition of molecular targets (six additional parameters) or tumor types (five additional parameters) to the final model resulted in OFV drops of 4.9 and 2.9, respectively, which are not significant ($P \gg 0.05$) considering the additional degrees of freedom added. The final model was also evaluated by case deletion diagnostics to investigate the influence of trial differences on the derived covariate relationships. Similar estimates of the covariate effects of prior PN and BWT were seen regardless of what trial was deleted from the data set (**Figure S3**). This suggests that the identified covariate relationships were not primarily driven by differences between individual trials.

Table 1. Parameter estimates of final model

Parameter (unit)	Description	Estimate	SE ^a	RSE ^b
Ktr (1/day)	Transit rate constant explaining delay in onset	0.0108		0.45
α	Drug effect parameter	0.0000619		0.51
β	Weibul function parameter	0.721		0.091
θ_{bwt} (1/kg)	Effect of BWT on hazard	0.0145	0.0042	
θ_{ppn}	Effect of prior PN on hazard	0.434	0.15	

BWT, body weight; PN, peripheral neuropathy; RSE, relative standard error; SE, standard error.

^aEffects of covariates are estimated in the normal domain and can be negative, thus SE is presented. ^bModel parameters α , β , Ktr, are shown on normal scale but were estimated in the log domain. The RSE presented is the SE of the logged parameter that is approximately equal to the RSE of the parameter on the normal domain.

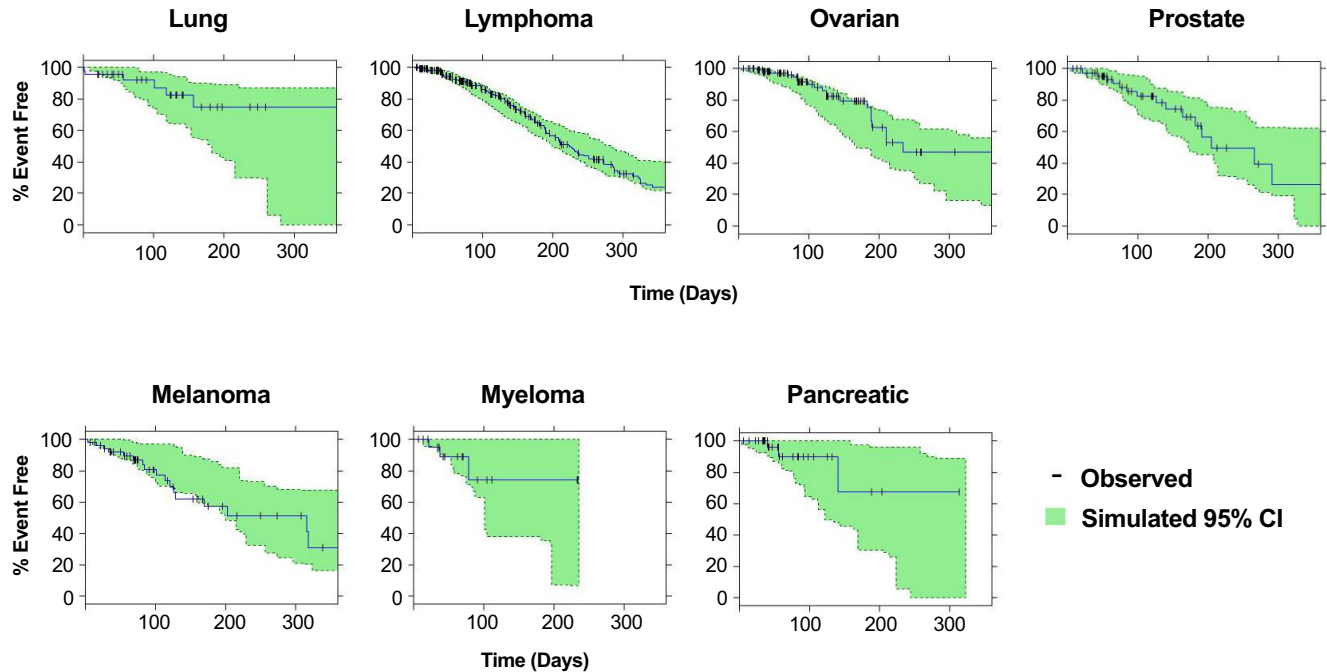


Figure 4. Kaplan–Meier visual predictive check for time to grade ≥ 2 peripheral neuropathy by cancer type. Based on the final model. CI, confidence interval.

The combined impact of dose, prior PN, BWT, and treatment duration on the risk for developing PN at cycles 8 or 12 is illustrated based on the final model in **Figure 5**.

Simulations were performed to explore dose capping and the flat dose as alternatives to dosing in proportion to BWT. As illustrated in **Figure 6**, capping the dose for heavy patients (>100 kg) only had a marginal benefit for the heaviest patients in terms of reduced PN risk compared with mg/kg dosing. When compared with BWT-based dosing (i.e., mg/kg), flat dosing did not change the overall risk for the population. It did, however, slightly increase the risk in lighter patients and slightly reduced the risk in the heavier patients. It should be noted that the risk was still higher in heavy patients despite lower plasma drug exposures resulting from flat dosing.

DISCUSSION

PN is commonly observed with chemotherapeutic agents targeting microtubules and is also one of the most common adverse events in patients treated with the vc-MMAE ADCs. A new or worsening grade ≥ 2 PN, according to NCI-Common Terminology Criteria for Adverse Events (CTCAE) v4.0, is considered clinically significant, resulting in diminished quality of life in patients, and may lead to off-therapy worsening of neurotoxic symptoms. It often necessitates dose interruptions, reductions, and/or early treatment discontinuations that in turn may have a negative impact on antitumor activity for potentially life-saving vc-MMAE ADCs. The availability of standardized data enabled the creation of an integrated data set (~700 patients) for the eight vc-MMAE ADCs across nine phase I and II clinical trials. This large database facilitated a comprehensive analysis that improved the understanding of the risk

for developing PN and the relation to dose and treatment duration. In addition, the influence of potential patient-specific demographic and pathophysiological factors on the development of the PN risk was assessed using the integrated data set.

The present analysis showed that the ac-MMAE in plasma approached steady-state concentrations within the first cycle upon repeated q3w dosing. The incidence of grade ≥ 2 PN was initially low and did not start to increase until around 60 days following administration of the study drug, with a median time to onset of ~200 days. This suggested that peripheral nerve damage develops gradually, with a delayed onset for the manifestation of the PN symptoms. An effect compartment was incorporated in the model to enable a delay between initiation of treatment and increased risk for developing of grade ≥ 2 PN. The present modeling approach was restricted to modeling the onset of clinically relevant grade ≥ 2 PN events. An understanding of the full-time course, i.e., onset and subsequent changes in severity and recovery of PN over time, would be of considerable interest to inform individual dose adjustments *a posteriori* to effectively manage the PN symptoms. However, given the limitations around the reliability of monitoring and reporting the severity of adverse event grade or resolution to the baseline grade in clinical trials, this was deemed not possible in the present analysis. To comprehensively characterize the time course of PN longitudinally, more focused efforts on the accurate recording of changes in adverse event grade are needed in the clinical assessment. Standardized clinical grading scales, patient-reported outcomes, and functional assessments focused on neuropathy could also be helpful in this respect.¹⁰

The observed exposure–response relationship was well captured by this model. It was explained using a linear

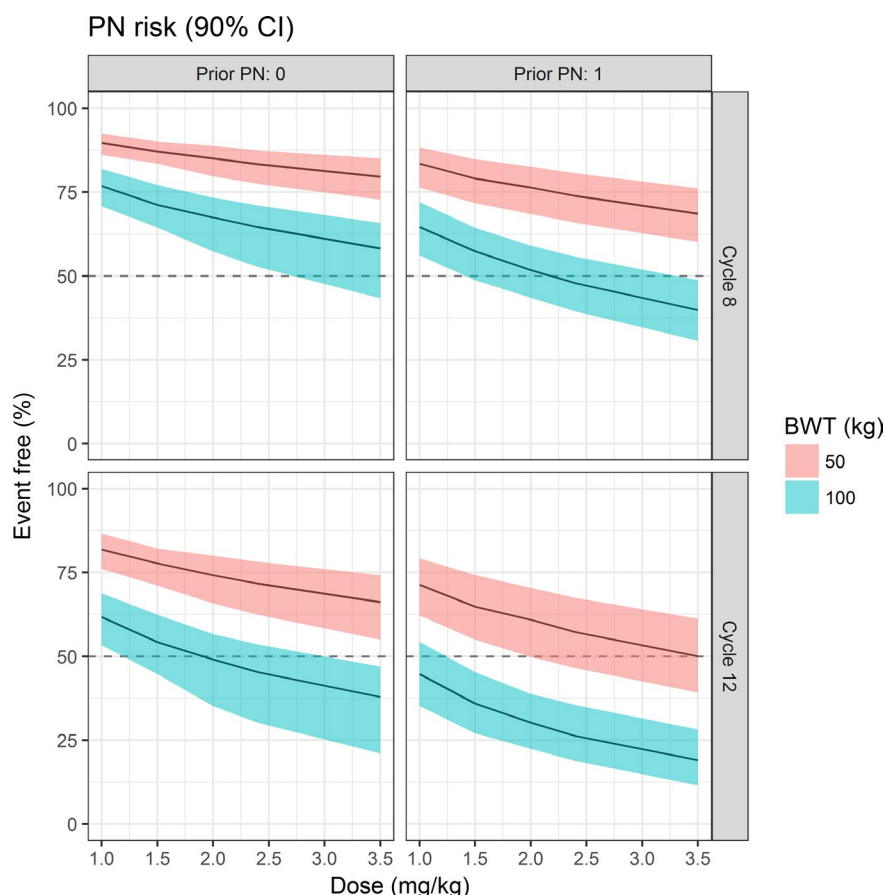


Figure 5. Model-predicted probability of being event free (grade ≥ 2 PN) at 8 and 12 cycles for patients given a dosing regimen every 3 weeks at doses ranging from 1–3.5 mg/kg. Predictions are derived for patients with a BWT of 50 kg and 100 kg without (0) or with (1) prior PN. Shaded areas are the 90% CI, derived based on a nonparametric bootstrap ($N = 200$). BWT, body weight; CI, confidence interval; PN, peripheral neuropathy.

relationship between the ac-MMAE concentration in the effect compartment and the hazard, suggesting a gradual increase in the risk for grade ≥ 2 PN with an increase in drug exposure. Furthermore, the availability of the base TTE model, including the time course of the ac-MMAE systemic exposure enabled exploration of covariate effects on the PN risk after accounting for any difference in exposure.

Two patient-specific factors that influenced the risk for grade ≥ 2 PN were identified in the covariate analysis: prior PN and BWT. The importance of these factors seems to be of similar magnitude (**Figure 3**). The finding regarding prior PN was in line with several previous reports showing that patients with a preexisting neuropathy, either hereditary or acquired, were more susceptible to chemotherapy-induced neuropathies.^{37–39} Also, it is likely that patients with preexisting peripheral neuropathies have persisting nerve damage and therefore may experience increased sensitivity for the manifestation/progression of PN symptoms upon reinstitution of subsequent neurotoxic therapies. The presence of prior PN was identified based on the patient reporting recorded at the time of study entry. It has been proposed that PN is underreported by patients and underrecognized by doctors.⁴⁰ A careful objective neurophysiological assessment suitable for clinical use at screening, i.e., before the initiation of the

ADC treatment, might be more reliable in identifying patients with preexisting peripheral neuropathies with an increased risk for developing PN.

BWT was the second identified covariate that influenced the risk for PN. Higher ADC plasma concentrations in heavier patients relative to lighter BWT patients were observed when dosing in proportion to BWT.²⁰ The increased exposure in heavier patients resulting from mg/kg dosing was, however, not sufficient to explain the impact of BWT on the risk for developing PN. Instead, BWT appeared to be a risk factor independent of drug exposure. In fact, the model predicts a higher incidence of grade 2 PN in heavy compared with light patients even when flat dosing (180 mg) was applied, despite the lower exposure in heavier patients (**Figure 6**). The inclusion of BWT in the model also explained the apparent gender effect observed during the univariate screening of the covariates during the model development, suggesting that the observed gender difference resulted from a difference in body size. Diabetes and obesity have been reported to be associated with PN risk in published studies⁴¹ and were also correlated to BWT. It was therefore of interest to explore if BMI and diabetes rather than BWT were responsible for the increased risk. Replacing BWT with BMI in the final model, however, resulted in a poorer fit based on objective function

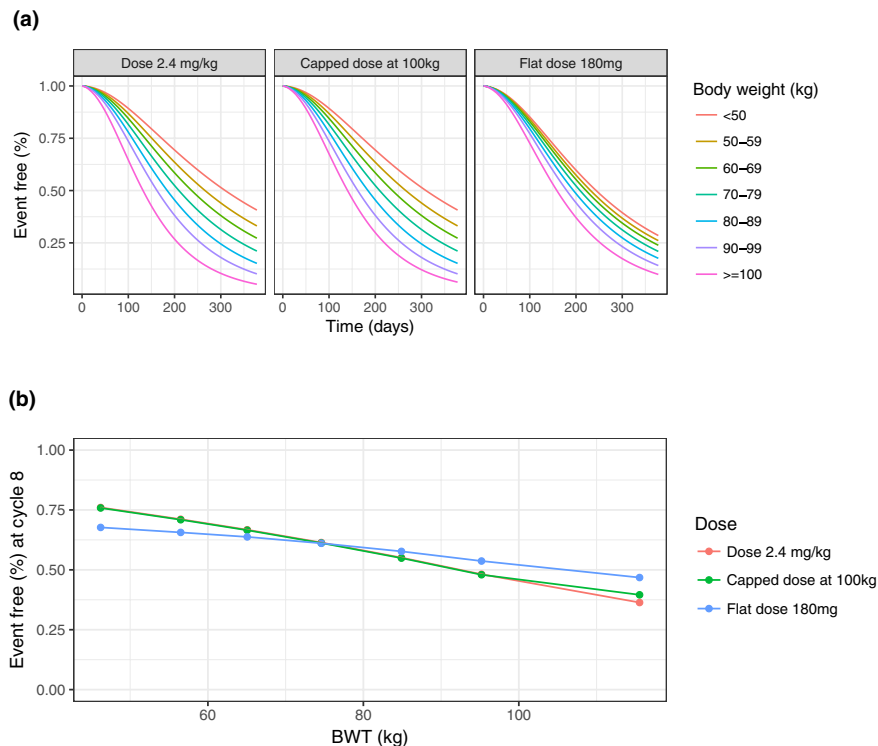


Figure 6. Influence of different body weight (BWT)-based dosing strategies on the probability of being event free vs. time (a) or vs. BWT at cycle 8 (b). Dosing strategies explored were 2.4, 2.4 mg/kg dosing but capping the dose at a BWT of 100 kg (dose = 240 mg), and flat dosing of 180 mg (2.4 mg/kg*75 kg) to all patients. All doses were given every 3 weeks. The simulations were based on patients with prior peripheral neuropathy and a BWT distribution similar to what was observed in the study. The simulation also accounted for the effect of BWT on the pharmacokinetics.

value and also could not explain the apparent gender effect. In addition, the estimated effect of BWT was not influenced by inclusion of diabetes as a covariate in the model. Hence, taken together, our analysis suggests that the increased risk associated with a high BWT may be related to the length and surface area of the axonal nerve fibers⁴² being available for the ADC exposure rather than obesity-induced inflammation or diabetes. It is also possible that a combination of these effects is in play.

After accounting for the dose, treatment duration, and covariates such as prior PN and BWT, no substantial differences in PN risk between the tested vc-MMAE ADCs/molecular targets/cancer types were identified, suggesting that the effect was nonspecific and not related to target or tumor type. The observed time to event was in the lower range predicted by the model for melanoma patients and in the upper range for ovarian patients. These trends may be the result of random variations between studies rather than an actual difference.

Following the evaluation of the performance of the developed TTE model for predicting PN risk, simulations were performed to evaluate (i) the impact of ADC dose and treatment duration on the incidence of PN risk in patients with and without the prior PN and (ii) the impact of flat, BWT-based dosing or dose capping to minimize the PN risk and/or inform clinical eligibility.

As illustrated in **Figure 6**, heavier patients with prior incidence of PN before treatment initiation are at a greater risk

of developing grade ≥ 2 PN following ADC administration, thereby warranting careful monitoring of PN symptoms in such patients. In addition, a shorter treatment duration (e.g., limited to eight cycles) or a lower dose intensity may be considered to reduce the risk of treatment induced PN.

Although flat dosing is not likely to reduce the overall PN incidence in the patient population as a whole, the simulations (**Figures 5 and 6**) suggest that it is possible to treat lighter weight patients for a longer duration and/or at a higher mg/kg dose when compared with heavier patients with acceptable risk for PN, thereby potentially improving efficacy in these patients. PN risk predictions for dose capping at 100 kg was comparable to the predicted PN risk following the administration of the BWT-based ADC dosing in the heavier patients. Hence, capping the dose at a BWT of 100 kg was likely to have a minimal impact on lowering the PN risk in the heavier patients (>100 kg) as illustrated in **Figure 6**.

In conclusion, a TTE model of PN was developed based on a large data set. It could be used to make predictions of the PN risk accounting for treatment duration, prior PN, and BWT, thus enabling an individualized dose/schedule selection for the vc-MMAE-containing ADCs. Our modeling effort was limited to the PN risk. A careful evaluation of the dose/schedule for individual molecules or patients also needs to consider efficacy as well as other safety aspects to optimize the benefit-risk balance of novel therapies for cancer patients.

Supporting Information. Supplementary information accompanies this paper on the *CPT: Pharmacometrics & Systems Pharmacology* website (www.psp-journal.com).

Figure S1. Kaplan–Meier visual predictive check illustrating goodness of fit for weekly (qw) and every 3 weeks (q3w) dosing.

Figure S2. Kaplan–Meier visual predictive check illustrating goodness of fit for patients with low (<75 kg) and high (≥75 kg) body weight (BWT) with and without prior peripheral neuropathy (PN).

Figure S3. Case deletion diagnostics by study based on final model. Estimated hazard ratios (95% CI) for BWT (upper figure) and Prior PN (lower figure). BWT, body weight; CI, confidence interval; PN, peripheral neuropathy.

Table S1. Parameter estimates of full model.

Table S2. Drug target, cancer type, and key covariate summary of the trials included in the analysis.

nonmem Model Code.

Data Set.

Acknowledgments. The authors acknowledge all investigators and patients for their participation and contribution to the clinical studies. Third-party writing assistance was provided by Anshin Biosolutions and funded by F. Hoffmann La Roche.

Funding. The analysis was funded by Genentech, Inc., a member of the Roche group.

Conflict of Interest. All authors, except W.G. are employees of Genentech, Inc. and stockholders of the Roche group. W.G. is a paid consultant for Roche and Genentech.

Author Contributions. M.K. and D.S. wrote the manuscript. M.K., D.S., D.L., C.L., J.Y.J., B.M.F., and S.G. designed the research. M.K., D.S., C.L., W.R.G., and J.Y.J. performed the research. M.K. and D.S. analyzed the data.

1. Howlader, N. *et al.* SEER cancer statistics review, 1975–2013 <https://seer.cancer.gov/csr/1975_2013/> (2016).
2. Cavaletti, G. & Zanna, C. Current status and future prospects for the treatment of chemotherapy-induced peripheral neurotoxicity. *Eur. J. Cancer* **38**, 1832–1837 (2002).
3. Wolf, S., Barton, D., Kottschade, L., Grothey, A. & Loprinzi, C. Chemotherapy-induced peripheral neuropathy: prevention and treatment strategies. *Eur. J. Cancer* **44**, 1507–1515 (2008).
4. Hilken, P.H. *et al.* Neurotoxicity is not enhanced by increased dose intensities of cisplatin administration. *Eur. J. Cancer* **31A**, 678–681 (1995).
5. Thompson, S.W., Davis, L.E., Kornfeld, M., Hilgers, R.D. & Standefer, J.C. Cisplatin neuropathy. Clinical, electrophysiologic, morphologic, and toxicologic studies. *Cancer* **54**, 1269–1275 (1984).
6. Kudlowitz, D. & Muggia, F. Defining risks of taxane neuropathy: insights from randomized clinical trials. *Clin. Cancer Res.* **19**, 4570–4577 (2013).
7. Peng, L., Bu, Z., Ye, X., Zhou, Y. & Zhao, Q. Incidence and risk of peripheral neuropathy with nab-paclitaxel in patients with cancer: a meta-analysis. *Eur. J. Cancer Care (Engl)*. <https://doi.org/10.1111/ecc.12407>. [e-pub ahead of print].
8. Kaplan, L.D., Deitcher, S.R., Silverman, J.A. & Morgan, G. Phase II study of vincristine sulfate liposome injection (Marqibo) and rituximab for patients with relapsed and refractory diffuse large B-Cell lymphoma or mantle cell lymphoma in need of palliative therapy. *Clin. Lymphoma Myeloma Leuk* **14**, 37–42 (2014).
9. Verstappen, C.C. *et al.* Dose-related vincristine-induced peripheral neuropathy with unexpected off-therapy worsening. *Neurology* **64**, 1076–1077 (2005).
10. Park, S.B. *et al.* Chemotherapy-induced peripheral neurotoxicity: a critical analysis. *CA Cancer J. Clin.* **63**, 419–437 (2013).
11. Hershman, D.L. *et al.* Prevention and management of chemotherapy-induced peripheral neuropathy in survivors of adult cancers: American Society of Clinical Oncology clinical practice guideline. *J. Clin. Oncol.* **32**, 1941–1967 (2014).
12. Cavaletti, G. *et al.* The chemotherapy-induced peripheral neuropathy outcome measures standardization study: from consensus to the first validity and reliability findings. *Ann. Oncol.* **24**, 454–462 (2013).

13. Stubblefield, M.D. *et al.* NCCN task force report: management of neuropathy in cancer. *J. Natl. Compr. Canc. Netw.* **7**(suppl. 5), S1–S26; quiz S27–S28 (2009).
14. Mullard, A. Maturing antibody-drug conjugate pipeline hits 30. *Nat. Rev. Drug Discov.* **12**, 329–332 (2013).
15. Beck, A., Goetsch, L., Dumontet, C. & Corvaia, N. Strategies and challenges for the next generation of antibody-drug conjugates. *Nat. Rev. Drug Discov.* **16**, 315–337 (2017).
16. Doronina, S.O. *et al.* Development of potent monoclonal antibody auristatin conjugates for cancer therapy. *Nat. Biotechnol.* **21**, 778–784 (2003).
17. Moskowitz, C.H. *et al.* Brentuximab vedotin as consolidation therapy after autologous stem-cell transplantation in patients with Hodgkin's lymphoma at risk of relapse or progression (AETHERA): a randomised, double-blind, placebo-controlled, phase 3 trial. *Lancet* **385**, 1853–1862 (2015).
18. Swain, S.M. & Arezzo, J.C. Neuropathy associated with microtubule inhibitors: diagnosis, incidence, and management. *Clin. Adv. Hematol. Oncol.* **6**, 455–467 (2008).
19. Younes, A. *et al.* Results of a pivotal phase II study of brentuximab vedotin for patients with relapsed or refractory Hodgkin's lymphoma. *J. Clin. Oncol.* **30**, 2183–2189 (2012).
20. Kagedal, M. *et al.* Platform model describing pharmacokinetic properties of vc-MMAE antibody-drug conjugates. *J. Pharmacokinet Pharmacodyn.* **44**, 537–548 (2017).
21. Advani, R.H. *et al.* Phase I study of the anti-CD22 antibody-drug conjugate pinatuzumab vedotin with/without rituximab in patients with relapsed/refractory B-cell non-Hodgkin lymphoma. *Clin. Cancer Res.* **23**, 1167–1176 (2017).
22. Burris, H.A. *et al.* A phase I study of DNIB0600A, an antibody-drug conjugate (ADC) targeting NaPi2b, in patients (pts) with non-small cell lung cancer (NSCLC) or platinum-resistant ovarian cancer (OC). *J. Clin. Oncol.* **32**, 2504 (2014).
23. Danila, D.C. *et al.* A phase I study of the safety and pharmacokinetics of DSTP3086S, an Anti-STEAP1 antibody-drug conjugate, in patients with metastatic castration-resistant Prostate cancer. American Society of Clinical Oncology Annual Meeting (May 31–June 4), Chicago, IL, 2013.
24. Li, C. *et al.* Clinical pharmacokinetics of EDN6526A, an anti-endothelin B Receptor (ETBR) antibody- drug conjugate (ADC) in patients (pts) with metastatic or unresectable melanoma: results from a first-in-human phase I study. American Association of Pharmaceutical Scientists National Biotechnology Conference (August 6–October 6), Orlando, FL, 2015.
25. Liu, J.F. *et al.* Phase I study of safety and pharmacokinetics of the anti-MUC16 antibody-drug conjugate DMUC5754A in patients with platinum-resistant ovarian cancer or unresectable pancreatic cancer. *Ann. Oncol.* **27**, 2124–2130 (2016).
26. Palanca-Wessels, M.C. *et al.* Safety and activity of the anti-CD79B antibody-drug conjugate polatuzumab vedotin in relapsed or refractory B-cell non-Hodgkin lymphoma and chronic lymphocytic leukaemia: a phase 1 study. *Lancet Oncol.* **16**, 704–715 (2015).
27. Stewart, A.K. *et al.* Phase I study of the anti-FcRH5 antibody-drug conjugate DFRF4539A in relapsed or refractory multiple myeloma. *Blood Cancer J.* **9**, 17 (2019).
28. Weekes, C.D. *et al.* Phase I study of DMOT4039A, an antibody-drug conjugate targeting mesothelin, in patients with unresectable pancreatic or platinum-resistant ovarian cancer. *Mol. Cancer Ther.* **15**, 439–447 (2016).
29. Food and Drug Administration. ADCETRIS, original BLA 125388 and 125399—Brentuximab vedotin (Center for Drug Evaluation and Research, 2011). Food and Drug Administration, Silver Spring, MD.
30. Lu, D. *et al.* Time-to-event analysis of polatuzumab vedotin-induced peripheral neuropathy to assist in the comparison of clinical dosing regimens. *CPT Pharmacometrics Syst. Pharmacol.* **6**, 401–408 (2017).
31. International Conference on Harmonisation. ICH guidelines <<https://www.ich.org/home.html>> (2005).
32. Kaur, S., Xu, K., Saad, O.M., Dere, R.C. & Carrasco-Triguero, M. Bioanalytical assay strategies for the development of antibody-drug conjugate biotherapeutics. *Bioanalysis* **5**, 201–226 (2013).
33. Beal, S.L., Sheiner, L.B., Boeckmann, A.J. & Bauer, R.J. NONMEM users guides 1989–2011 (Icon Development Solutions, Elliot City, MD, 2011).
34. Keizer, R.J., Karlsson, M.O. & Hooker, A. Modeling and simulation workbook for NONMEM: tutorial on Pirana, PsN, and Xpose. *CPT Pharmacometrics Syst. Pharmacol.* **2**, e50 (2013).
35. Gastonguay, M.R. Full covariate models as an alternative to methods relying on statistical significance for inferences about covariate effects: a review of methodology and 42 case studies. *AAPS J* **6**, W4354 (2004).
36. Papanas, N. & Ziegler, D. Risk factors and comorbidities in diabetic neuropathy: an update 2015. *Rev. Diabet. Stud.* **12**, 48–62 (2015).
37. Chaudhry, V., Chaudhry, M., Crawford, T.O., Simmons-O'Brien, E. & Griffin, J.W. Toxic neuropathy in patients with pre-existing neuropathy. *Neurology* **60**, 337–340 (2003).

38. Kalfakis, N. *et al.* Hereditary neuropathy with liability to pressure palsies emerging during vincristine treatment. *Neurology* **59**, 1470–1471 (2002).
39. Trobaugh-Lotrario, A.D., Smith, A.A. & Odom, L.F. Vincristine neurotoxicity in the presence of hereditary neuropathy. *Med. Pediatr. Oncol.* **40**, 39–43 (2003).
40. Velasco, R. & Bruna, J. Chemotherapy-induced peripheral neuropathy: an unresolved issue. *Neurologia* **25**, 116–131 (2010).
41. Smith, E.M., Beck, S.L. & Cohen, J. The total neuropathy score: a tool for measuring chemotherapy-induced peripheral neuropathy. *Oncol. Nurs. Forum* **35**, 96–102 (2008).
42. Kote, G.S., Bhat, A.N., Ismail, M.H. & Gupta, A.. Peripheral insensate neuropathy-is height a risk factor? *J. Clin. Diagn. Res.* **7**, 296–301 (2013).

© 2019 Genentech Inc. *CPT: Pharmacometrics & Systems Pharmacology* published by Wiley Periodicals, Inc. on behalf of the American Society for Clinical Pharmacology & Therapeutics. This is an open access article under the terms of the Creative Commons Attribution-NonCommercial-NoDerivs License, which permits use and distribution in any medium, provided the original work is properly cited, the use is non-commercial and no modifications or adaptations are made.